Supplementary Information

Constructing Polyamide/Ceramic Composite Membranes for Highly Efficient and Selective Separation towards Dye/salt Solution

Yujie Zang,[a] Linlin Yan,[a] Tieying Yang,[a] Kai Wang,[a] Yingjie Zhang,[a,b] Enrico Drioli,[c] Jun Ma,[a,d] Yonggang Li,*[e] Shanshan Ji,*[f] Xiquan Cheng,*[a,b]

[a] State Key Laboratory of Urban Water Resource and Environment, School of Marine Science and Technology, Harbin Institute of Technology, Weihai 264209, P.R. China.

[b] Shandong Sino-European Membrane Technology Research Institute Co., Ltd., Weihai Key Laboratory of Water Treatment and Membrane Technology, Weihai 264209, P.R. China.

[c] Institute on Membrane Technology (ITM-CNR), Via P. Bucci 17c, 87036 Rende, CS, Italy.

[d] School of Environmental Science and Engineering, Harbin Institute of Technology, Harbin 150001, P.R. China.

[e] Guangxi Key Laboratory of Urban Water Environment, Baise University, Baise 533000, China

[f] Department of Biological and Chemical Engineering, Jining Polytechnic, Jining, 272037, China.

*Correspondence should be directed to Prof. X. Q. Cheng (chengxiquan@hit.edu.cn) and Dr. S. Ji (ansirain@163.com).

Contents

1. Characterization of the TFC membrane

Surface morphologies. The microstructures of the prepared membranes were characterized with a scanning electron microscope (MERLIN Compact, Zeiss Company) after being coated with gold. The surface roughness and 3D structure of the ceramic support and PA/ceramic membrane were studied by a confocal laser scanning microscopy (CLSM). Moreover, the surface roughness and 3D structure of the commercial NF membranes were measured by an Atomic Force Microscopy (Bruker, Germany). To evaluate the roughness as precise as possible, three samples were characterized at least and the average values were calculated with error below 10%.

Chemical structure. The surface chemical composition and structure of the composite membranes were characterized by Fourier Transform Infrared Spectroscopy (Bruker TENSOR 27 spectrometer). As for XPS characterization, Mg Kα was used as the source of emission, the degree of vacuum was kept around 6×10^{-9} mbar, and data was obtained by using the SPECTRA version 8 operating system.

Surface properties. The Surface Analyzer (Surpass, Anton Paar GmbH) was used to characterize the surface zeta potential of ceramic support, PA/ceramic membrane and two types of commercial NF membranes. The hydrophilicity of the four membranes described above was measured by contact angle test equipment (SL200B/K Kino, America).

Separation performance. The concentration of salt solution was measured by electric conductivity meter (STARTER3100C, Shanghai Ohaus, China). The concentration of dye solution was determined by ultraviolet–visible spectrum apparatus (TU-1810, Beijing Puxi General Instrument Co., Ltd.).

2. The optimization of fabricated conditions for original PA/ceramic membranes

The effect of reaction time was firstly investigated. As shown in Figure S1a, with the increase of reaction polymerization time, the permeation flux of pure ethanol showed a trend of first increasing and then decreasing, while the BB retention had remained stable. The ultra-high retention rate of BB by composite membrane indicated that a relatively dense active separation layer has been formed on the surface of ceramic membrane. As the reaction time increases from 1 min to 3 min, the permeation flux of pure ethanol increased to a maximum of 1262.1 L m^{-2} h^{-1} bar^{-1}. This could be attributed to the polyamide pore structure caused by interfacial degassing of CO_2 due to the release of more H^+ and heat, as the polymerization reaction proceeded further[1, 2]. Besides, the release of heat during the IP process can also cause interfacial evaporation of volatile organic solvents. When the reaction time exceeded 3 min, the two monomers react sufficiently to form a denser polyamide selection layer, which reduced the ethanol permeation flux. Thus, considering the permeability and interception performance, the reaction time of 3 min is considered as an optimal reaction time.

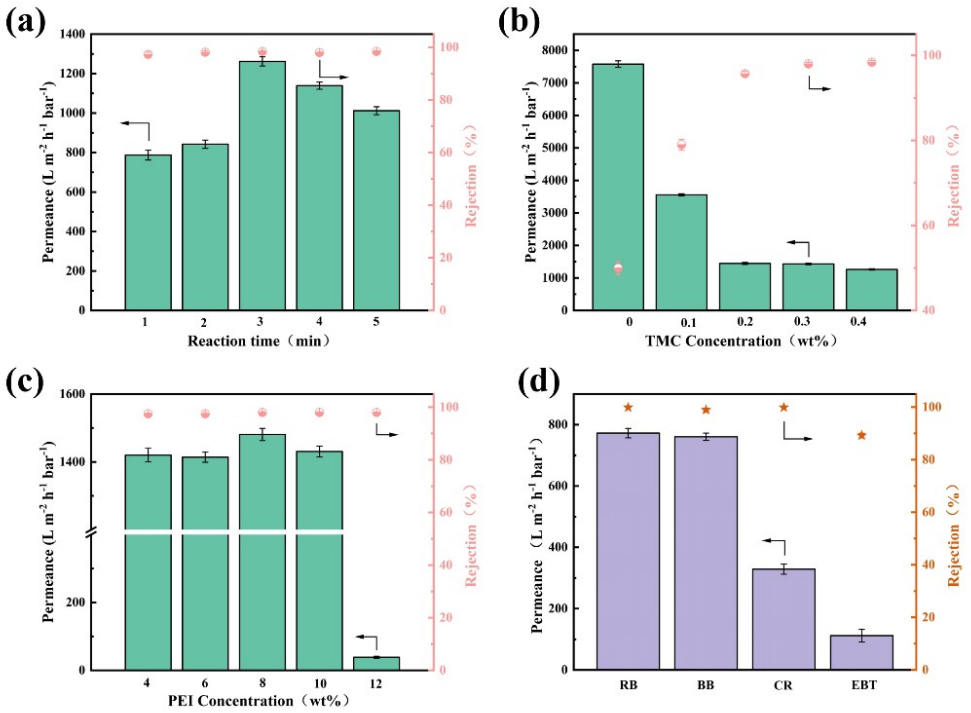

Fig. S1. The effects of the fabricated conditions on the separation performance of original polyamide/ceramic membrane: (a) reaction time; (b) TMC concentration; (c) PEI concentration;(d) the permeance and rejection of the TFC membranes toward different dyes in ethanol.

The TFC membranes were prepared by different TMC concentration and PEI concentration, and the corresponding separation properties were presented in Fig. S1b and Fig. 1c. It can be seen that the permeability of composite membrane decreased with the increase of TMC concentration and finally tended to stabilize, while the retention was just the opposite. When the TMC concentrations were less than 0.3 wt%, the amount of acid chloride monomer is relatively insufficient with that of amine monomer. PEI monomers was not sufficiently polymerized, making it difficult for the active separation layer to form defect-free dense network macromolecules. When the TMC concentration reached 0.3 wt%, a complete active separation layer had been formed on the ceramic surface, so the performance of the TFC membrane no longer changed even if the TMC concentration increased. Similarly, the trend of PEI concentration can be obtained. As presented in Fig. S1c, PEI concentration ranging from 4 wt% to 10 wt% had no measurable effect on permeate flux or BB rejection. However, the permeation flux decreased to a large extent at a PEI concentration of 12 wt%, which might be due to the high viscosity at a higher PEI concentration and the agglomeration of polyamide

molecules. From all results, the TFC membrane prepared with TMC concentration of 0.3 wt% in organic phase and PEI concentration of 8 wt% exhibits optimal properties including high ethanol permeance flux and dye rejection. The interception effect of the membrane prepared under this condition on different dyes in ethanol is shown in the Fig. S1d. The TFC membrane separated well in the dye-ethanol system, which confirmed its suitability for organic solvents.

3. Supplementary Figures

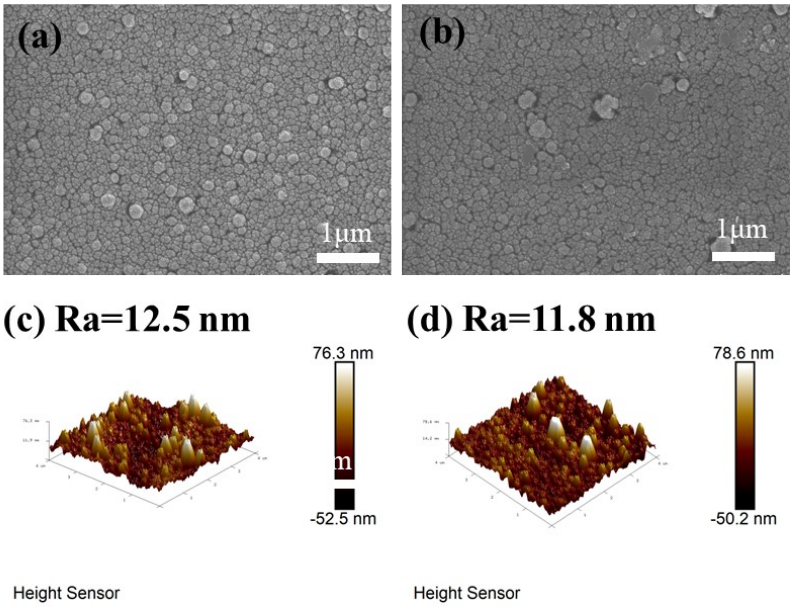

Fig. S2. (a) and (b) scanning electron micrographs (top view) of GC-1 and GC-2; (c) and (d) AFM images of the GC-1 and GC-2.

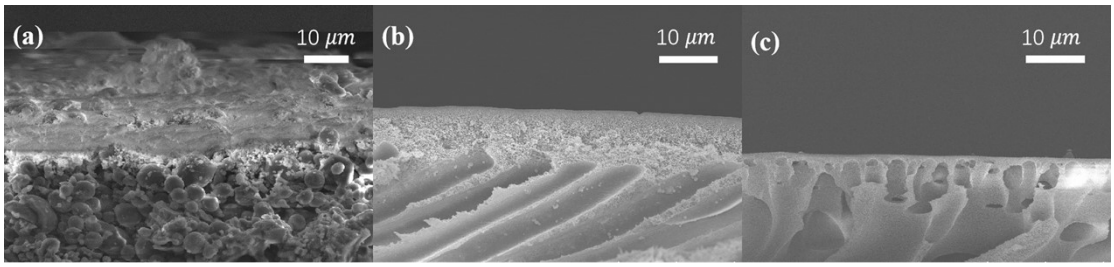

Fig. S3. Cross-section SEM images of (a) PA/ceramic membrane, (b)GC-1, (c) GC-2.

4. Adsorption capacity testing

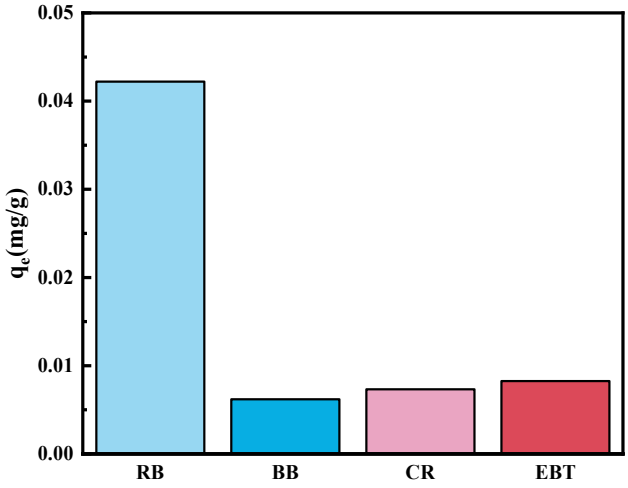

Fig. S4. Adsorption capacity of composite membranes for dyes of different molecular weights.

5. Dye molecular structures

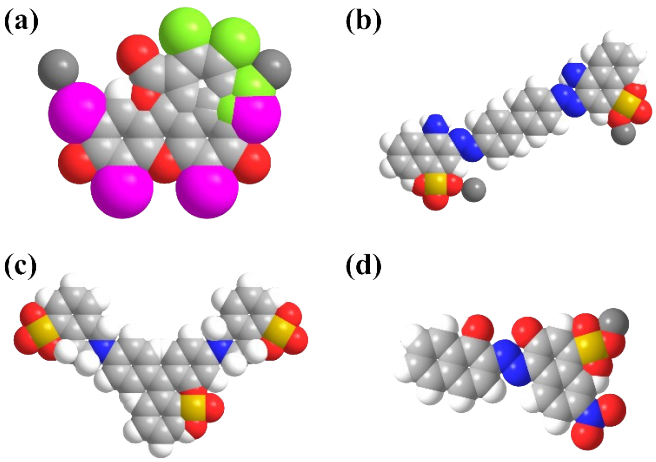

Fig. S5. Simulation of dye molecular structures: (a)RB(b)CR(c)BB(d)EBT

6. Long-time operation stability

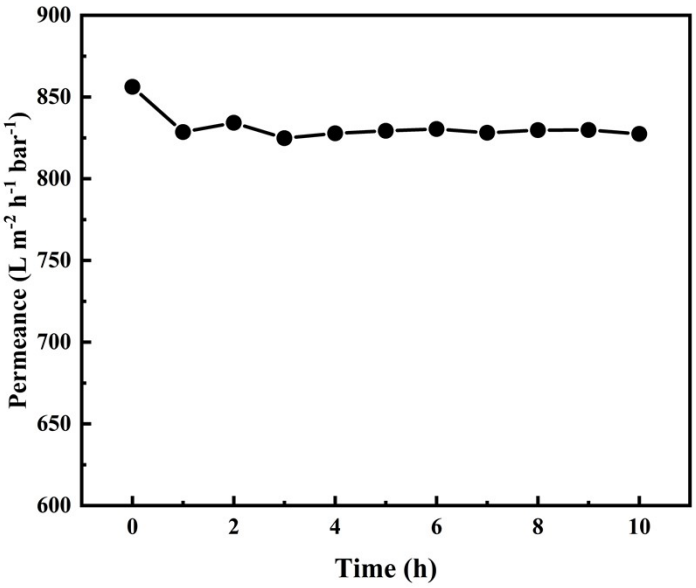

Fig. S6. Long-term stability of the composite membranes in pure water

7. Notes and references

[1] Ma, X.-H.; Yao, Z.-K.; Yang, Z.; Guo, H.; Xu, Z.-L.; Tang, C. Y.; Elimelech, M., Nanofoaming of Polyamide Desalination Membranes To Tune Permeability and Selectivity. *Environmental Science & Technology Letters*, 2018, 5(2), 123-130.

[2] Ma, X.; Yang, Z.; Yao, Z.; Guo, H.; Xu, Z.; Tang, C. Y., Tuning roughness features of thin film composite polyamide membranes for simultaneously enhanced permeability, selectivity and anti-fouling performance. *JOURNAL OF COLLOID AND INTERFACE SCIENCE*, 2019, 540, 382-388.